Hindawi
International Journal of Polymer Science
Volume 2019, Article ID 5409821, 9 pages
https://doi.org/10.1155/2019/5409821

Research Article

Characterization of Rice Husk Fiber-Reinforced Polyvinyl Chloride Composites under Accelerated Simulated Soil Conditions

Lei Wang and Chunxia He

College of Engineering, Nanjing Agricultural University, Nanjing 210031, China

Correspondence should be addressed to Chunxia He; chunxiahe@hotmail.com

Received 16 November 2018; Accepted 27 January 2019; Published 17 April 2019

Academic Editor: Domenico Acierno

To study the effect of accelerated simulated soil aging on the physical, mechanical, and thermal behavior of rice husk fiber-reinforced polyvinyl chloride composites. The worst soil aging condition was determined using the orthogonal design method, and the physical, mechanical, and thermal properties of the composites were analyzed over 21 d. The results indicate that the worst soil-accelerated aging condition was as follows: soil temperature of 65°C, soil pH of 2.5, soil moisture content of 45%, and soil porosity (ratio of thick to thin) of 3 : 7. An extended aging time tends to cause poor interfacial bonding quality, and the presence of many microcracks reduced thermal stability and flexural and impact strength. Many fibers were exposed, which resulted in increasing 24 h water absorption and thermal expansion coefficient. The hardness, tensile strength, flexural strength, impact strength, and pyrolysis temperature of the composites (after 21 d of aging) decreased from 50 HRR, 17.42 MPa, 35.2 MPa, 3.19 kJ/m^2, and 258.5°C to 26 HRR, 11.5 MPa, 16.8 MPa, 1.16 kJ/m^2, and 251.3°C, respectively. The mass loss rate, 24 h water absorption, discoloration, and line thermal expansion coefficient of the composites increased from 0%, 4.19%, 0, and 28.43 to 2.9%, 7.92%, 29.03, and 29.98, respectively.

1. Introduction

Wood-plastic composites (WPCs) are made of plant fiber and thermoplastic resin and have many advantages of moisture, pest, and fire resistance [1–5]; thus, these materials are often applied to industrial construction, garden facilities, and environmental protection [6–8].

Many studies have focused on the aging of composites under different conditions, such as xenon lamp aging [9, 10], ultraviolet aging [11, 12], bacterial aging [13, 14], and seawater and acid rain aging [15, 16]. Soil aging is a common aging type, and improving aging resistance is significant for the application of composites [17, 18]. It is rare to study the service performance under the accelerated soil aging condition. The degradation of silica-reinforced composites (rubber/silica) in soil and under UV radiation was studied, revealing that 20 wt% silica can improve the aging resistance and dispersion of composites [19]. The effect of soil aging was related to the service life of composites; long soil aging can degrade their mechanical properties [20–22]. Thus, it is necessary to improve the antiaging ability of composites.

An orthogonal experiment of four factors (the soil moisture, temperature, pH value, and soil porosity) and three levels was performed, with the particle size ratio of diatomite as the test level. The experimental data were analyzed to determine the worst aging conditions. The physical (mass loss rate, 24 h water absorption, discoloration, and hardness), mechanical (tensile, flexural, and impact strength), and thermal (line thermal expansion coefficient and thermogravimetric curves) properties of the composites were analyzed.

2. Experiment

2.1. Materials. Rice husk fibers (RHF), H-108 PE wax, and nontoxic 603 Ca/Zn composite stabilizers were purchased from Hebei Pengyue Minerals Trading Co. Ltd., China. SG-5 PVC (100 meshes) was purchased from Wenzhou Zhengbang Chemical Co. Ltd., China. Maleic anhydride-grafted

Table 1: Chemical reagent usage.

Chemical reagents	NaCl	Na_2SO_4	$MgSO_4$	$CaCl_2$	KNO_3	$NaHCO_3$
Content (g/L)	0.23	0.07	0.09	0.05	0.33	0.07

PVC was purchased from Shenzhen Hai'an Plastic Chemical Co. Ltd., China. Diatomite (20-40 and 200 meshes) was purchased from the Shenzhen Haiyang Powder official flagship store. Chemical reagents (NaCl, Na_2SO_4, $MgSO_4$, $CaCl_2$, KNO_3, and $NaHCO_3$) were purchased from Nanjing Chemical Reagent Co. Ltd., China.

2.2. Preparation of the PVC/RHF Composites. First, RHF powder (149 μm pore size) was dried in a DHG-9140A electrothermostatic drum wind drying oven (Nanjing Dongmai Scientific Instrument Co. Ltd., China) set at 90°C for 12 h. The contents of the stabilizer, the PE wax, and the maleic anhydride-grafted PVC were selected as 8, 5, and 3 wt%, respectively. The polymer was placed into an SBH-5L three-dimensional (3D) linkage mixer (Nanjing Xinbao Mechanical and Electrical Industry Co. Ltd., China). The PVC/RHF (at the proportion of 1 : 1) composites were prepared at 20 rpm using an RM-200C conical twin-screw extruder (Harbin Hapro Electric Technology Co. Ltd., China). The extrusion processing temperature for the composites was controlled between 150 and 165°C. A specially designed sample with a size of $100 \times 10 \times 7$ mm was obtained.

2.3. Accelerated Experiment Procedure of Simulated Soil Aging. To simulate the situation of soil burial accurately, we referred to ASTM G160 (2012) for the accelerated experiment of simulated soil aging. The average pH value of the soil of Jiangsu Province was 3.5–5.4 [23]. When acid rain occurred, the pH of the soil could be reduced, and the minimum pH in this period reached approximately 2.5. The accelerated experiment was divided into three main stages. In the first stage, diatomite was selected at different porosity ratios, and the particle sizes of 20-40 and 200 meshes were alternately mixed. The diatomite was placed into an LHS-80HC-I humidity alternating tester (Shanghai Yiheng Scientific Instruments Co. Ltd., China), and the humidity was set at 90% for 7 d. In the second stage, the solution was prepared with different pH values, and chemical reagents were added (Table 1). To accelerate the period of soil aging, chemical reagents of the simulated soil were added to the real soil at a mass ratio of 5 : 1. In the third stage, diatomite and the soil-mineral solution were mixed uniformly [24, 25]. The experimental period was chosen as 7, 14, and 21 d, respectively.

2.4. Experimental Procedure. To study the effect of simulated soil aging on the biodegradation performance of the WPCs, the experiment of the simulated soil was divided into two main stages. In the first stage, the orthogonal design was selected according to the $L_9(3^4)$ orthogonal table, which mainly included four factors: soil temperature (X_1), soil pH value (X_2), soil moisture content (X_3), and soil porosity (ratio of thick and thin) (X_4) (see Table 2 for the experimental factor level). The cut-off period was 7 d, and the aim of the measurement was to study the flexural strength. The Design-Expert software was used to identify the worst soil aging parameters. In the second stage, the biodegradation performance was analyzed for the worst aging parameters applied to the aging samples for three periods (i.e., 21 d).

Table 2: Factors and levels of orthogonal experiment.

Treatment no.	X_1 (°C)	X_2	X_3 (%)	X_4
Level 1	35	2.5	25	3 : 7
Level 2	50	3.5	35	5 : 5
Level 3	65	4.5	45	7 : 3

For the experiment, deionized water served as the mother liquor, which was used to adjust the chemical reagents to a certain salinity level (see Table 1). Considering the actual situation of Jiangsu Province of China [26], the maximum land surface temperature can reach almost 70°C; thus, the soil temperature was selected in the range of 35–65°C. We analyzed the characteristics of the soil in Jiangsu Province in a special environment where acid rain often occurs. There was severe causticity in the soil with acid rain, which was harmful for the outdoor composite materials. According to this situation, the soil pH value and moisture content were selected as 2.5, 3.5, and 4.5 and 25%, 35%, and 45%, respectively. The soil porosity was selected as 3 : 7, 5 : 5, and 7 : 3 according to the actual situation in the soil.

2.5. Characterization. The aging was performed via full immersion. A total of 1 L of the simulated soil solution was added to the beakers, and the PVC/RHF composite samples were buried at a depth of 10 cm under the simulated soil surface. To avoid water evaporation, the beakers were covered with a plastic wrap and placed on an HH-600 thermostatic water tank (Shanghai Baidian Instrument Equipment Co. Ltd., China) at a soil temperature. The experimental fluctuations were kept below 1°C. When the experiment was finished, the samples were removed from the solution and air-dried until they reached a stable mass (mass variation < 1%). The biodegradation behavior of the samples was evaluated.

2.5.1. Physical and Mechanical Properties of the Composites. Water absorption (WA) tests were performed in accordance with the Chinese standard GB/T 17657 (2013) by using an HH-600 thermostatic water tank (Shanghai Baidian Instrument Equipment Co. Ltd., China). The dried samples were immersed in deionized water at a temperature of 23 ± 1°C. The immersed samples were reweighed after 24 h.

The water absorption was in accordance with the following equation.

$$c = \frac{W_1 - W_0}{W_0} \times 100\%. \quad (1)$$

Here, W_0 and W_1 indicate the dried weight and the immersed weight after 24 h, respectively.

The tensile, flexural, and impact properties of the composites were evaluated in accordance with the Chinese standards GB/T 1040.4 (2006), GB/T 9341(2008), and GB/T 1043.1 (2008), respectively, using a CMT6104 electronic universal testing machine (MTS Industrial Systems Co. Ltd., China). The speed and test temperature were set as 2 mm/min and room temperature, respectively.

The weight loss (WL) rate represented the weight variation of the composites after soil aging and was in accordance with the following equation.

$$\mathrm{WL} = \frac{W_1 - W_2}{W_1} \times 100\%. \quad (2)$$

Here, W_1 and W_2 indicate the weights of the composites before and after soil aging, respectively.

Chromatic aberration tests were performed using an HP-200 precise color reader (Shanghai Chinaspec Optoelectronics Technology Co. Ltd., China), in accordance with the CIE 1976 (L*a*b*) color space. The chromatic aberration tests were in accordance with the following equation.

$$\Delta E = \sqrt{\Delta L^2 + \Delta a^2 + \Delta b^2}. \quad (3)$$

Here, ΔE, ΔL, Δa, and Δb represent the discoloration, the color lightness, the color range from red ($\Delta a+$) to green ($\Delta a-$), and the color range from yellow ($\Delta b+$) to blue ($\Delta b-$).

Hardness tests were performed in accordance with the Chinese standard GB/T 3398.1 (2008) by using an XHR-150 plastic Rockwell hardness tester (Shanghai Joint Seoul Test Equipment Co. Ltd., China), as well as an HRR ruler. The time interval of the load was 5 s, the indenter diameter was selected as 12.7 mm, and the time of unloading was controlled at 15 s.

The average for five independent tests at room temperature (25 ± 1°C) was calculated.

2.5.2. Thermal Properties of the Composites. As a thermogravimetric analyzer (TGA), an STA 449 F3 synchronized thermal analyzer (Netzsch Scientific Instrument Trading Co. Ltd., Germany) was employed to analyze the decomposition temperature of the composites. Almost 10 mg of samples was placed in an Al_2O_3 crucible. The TGA was used in the heating range of 30 to 800°C at a rate of 20°C/min, and the test was performed in an argon atmosphere.

The linear coefficient of thermal expansion (LCTE) was determined using a PCY-D low-temperature expansion tester (Xiangtan Xiangyi Instrument Co. Ltd., Germany). Samples with a length, width, and thickness of 100, 10, and 7 mm, respectively, were used. The test temperature was controlled in the range of -30 to 60°C. The LCTE was obtained using the Universal TA analysis software as follows.

$$\mathrm{LCTE} = \frac{1}{L}\frac{dL}{dT}. \quad (4)$$

2.5.3. Fourier-Transform Infrared and Microscopic Structure. The Fourier-transform infrared (FTIR) photoacoustic spectra were recorded using a Nicolet iS10 FTIR spectrometer (Thermo Fisher Scientific Co. Ltd., China). The facilities were determined in the range of 400–4,000 cm^{-1} at a resolution of 4 cm^{-1}. There were 16 scans to collect in the absorbance mode.

A morphological analysis of the composites was performed using an S-4800 scanning electron microscope (Hitachi Ltd., Japan). Before the scanning electron microscopy (SEM) observation, gold sputtering of the composites was performed using an E-1010 ion sputter coater.

Table 3: Schemes and results of the orthogonal experiment.

Sample ID	X_1	X_2	X_3	X_4	Flexural strength (MPa)
L_1	1	1	1	1	17.5 ± 0.3
L_2	1	2	2	2	16.5 ± 0.6
L_3	1	3	3	3	15.3 ± 0.8
L_4	2	1	2	3	21.0 ± 0.3
L_5	2	2	3	1	21.3 ± 0.4
L_6	2	3	1	2	14.5 ± 0.9
L_7	3	1	3	2	25.1 ± 0.1
L_8	3	2	1	3	19.9 ± 0.3
L_9	3	3	2	1	20.7 ± 0.3

Table 4: Variance analysis of the orthogonal experiment.

Source	Sum of square	df	Mean square	F	Sig
Corrected model	277.707[a]	8	34.713	133.513	0.0
Intercept	9,838.413	1	9838.413	37,840.051	0.0
X_1	134.807	2	67.403	259.244	0.0
X_2	86.087	2	43.043	165.551	0.0
X_3	49.327	2	24.663	94.859	0.0
X_4	7.487	2	3.743	14.397	0.0
Error	4.680	18	0.260		
Total	10,120.800	27			
Corrected total	282.387	26			

[a]$R^2 = 0.98$ (adjusted $R^2 = 0.97$).

3. Results and Discussion

3.1. Analysis of Orthogonal Experiment Results. Table 2 shows the factors and levels of the orthogonal experiment, and the schemes and variance analysis of the orthogonal experiment are shown in Tables 3 and 4, respectively. According to the

Table 5: Mean and standard deviation for the orthogonal experiment.

Treatment no.	X_1	X_2	X_3	X_4
Level 1	16.4 ± 1.0^{c}	21.2 ± 3.3^{b}	17.3 ± 2.4^{b}	19.8 ± 1.8^{a}
Level 2	18.9 ± 3.4^{b}	19.2 ± 2.1^{ab}	19.4 ± 2.2^{ab}	18.7 ± 4.9^{a}
Level 3	21.9 ± 2.4^{a}	16.8 ± 2.9^{a}	20.5 ± 4.3^{a}	18.8 ± 2.7^{a}

Note: different superscripts represent significant differences in the data.

results, the P values of the four factors were lower than 0.01, indicating that the four factors are significant for the soil aging properties of the composites. Obviously, in Table 5, we can conclude that the worst soil aging combination is $X_{13}X_{21}X_{33}X_{41}$ at the experimental test of the flexural strength. In view of the actual situation of the outdoor environment in Jiangsu Province, the worst soil aging condition can occur in a special environment and seriously damage the service life of the composites. From Tables 3 and 4, we draw the conclusion that X_1 has the highest F value (259.244), followed by X_2 (165.551), X_3 (94.859), and X_4 (14.397). This indicates that the temperature has the largest influence on soil aging, followed by the pH value, soil moisture content, and soil porosity.

3.2. Chromatic Aberration, Mass Loss Rate, and 24 h Water Absorption of the Composites. It is well known that the service performance of the composites depends on the combined quality of the fiber and the matrix, and good interfacial combination can result in small diversification in chromatic aberration and minimal water absorption [27]. Figure 1 shows the mass variation, the discoloration, and the 24 h water absorption of the composites under accelerated soil aging. By analyzing the information, we draw the conclusion that the 24 h water absorption and discoloration of the composites increased from 4.19% and 0 to 7.92% and 29.03, respectively. The fibers swelled when they began to contact the water molecules; the resulting shear stress made it difficult for the matrix to form an ideal coating for the fibers (shown by the microcracks observed in Figure 2), the fiber-matrix interlocking strength was reduced, and more water-soluble pigments dissolved in the water. The poor encapsulation quality of the interface may cause the carbonyl group of the fibers to be exposed; the oxidation product (keto alkane) was conjugated to form a double-bond group (chromophore group) with a benzene ring, thereby aggravating the discoloration [28]. However, the accelerated simulated soil aging could not enhance the vibrational strength of the conjugated carbonyl (almost 1637 cm^{-1}) and the double-bond bending vibration (100-670 cm^{-1}). Visual evidence can be observed in Figure 3; these observations indicate that the effect of the chromophore group on the apparent chromatic aberration can be ignored.

The weight loss rate of the aged samples (21 d) was 2.9%, compared with the nonaged samples. This may be due to the cancellation of noncellulose substances (hemicellulose and lignin) in the fibers, which suffered in the special environment (high temperature, acid environment, and water immersion), similar to acid immersion treatment. This phenomenon can be observed by FTIR. Jiang et al. drew a similar conclusion for composites [15].

The reduction of the mass loss rate can be better explained by the 24 h water absorption, chromatic aberration, and interfacial adhesion of the composites which can be observed in Figure 2. The tight interfacial adhesion was clearly observed (Figure 2(a)), and the interface of the composites was blurred. The fiber was coated with the polymer matrix. When the composites were immersed into the soil (high temperature and moisture), the interface of the composites was clearly visible and the interfacial adhesion of the fiber and matrix was weakened (Figure 2(b)). The interfacial adhesion not only affected the physical performance of the composites but also had a negative influence on their mechanical and thermal properties.

3.3. FTIR Analysis of the PVC/RHF Composites. The FTIR spectra of the surface of aged and nonaged samples were observed, as shown in Figure 3. The typical peaks were as follows. Peaks at 3,420–3,410 cm^{-1} represent the –OH stretching vibration in cellulose and hemicellulose, and the –OH groups were found to decrease with increasing soil aging time; more fibers began to contact the external environment, indicating that water-induced swelling of the fibers led to the disappearance of hemicellulose and lignin (similar to hydrothermal treatment), and the two-phase interfacial adhesion became weaker. Asymmetric stretching vibration peaks at 2,930–2,850 cm^{-1} most likely represent the C-H in cellulose. The peaks observed at 1,745–1,710 cm^{-1} are attributed to the stretching vibration of C-O in lignin and hemicellulose. The typical peaks at 1,250–1,230 cm^{-1} correspond to the stretching vibration in lignin. The peaks at 1,100–990 cm^{-1} are probably due to the C-O stretching vibration in polysaccharide. The peaks at 700-600 cm^{-1} are probably due to the C-Cl vibration band in polyvinyl chloride (PVC). The peaks (700-600 cm^{-1}) for different aging times had no obvious difference, indicating that the C-Cl group in the PVC molecular chain was not destroyed.

There is no doubt that for similar chemical groups in different aging periods, the samples were not chemically changed by the accelerating soil aging, indicating that the chemical functional groups did not affect the performance of the composites. This result is similar to that of Wang et al. [29] who studied the preparation and characterization of PVC matrix composites.

3.4. Physical and Mechanical Properties of the PVC/RHF Composites. The physical and mechanical properties of the composites significantly affect their practical application. The PVC/RHF composites had different physical and mechanical properties with different aging periods; the overall trend curves are shown in Figure 4. The hardness and the tensile, flexural, and impact strength of the composites (after 21 d of aging) decreased from 50 HRR, 17.42 MPa, 35.2 MPa, and 3.19 kJ/m^2 to 26 HRR, 11.5 MPa, 16.8 MPa, and 1.16 kJ/m^2, respectively, compared with those of the nonaged materials. Accelerated soil aging caused internal damage to the WPCs; the appearance of microcracks can limit

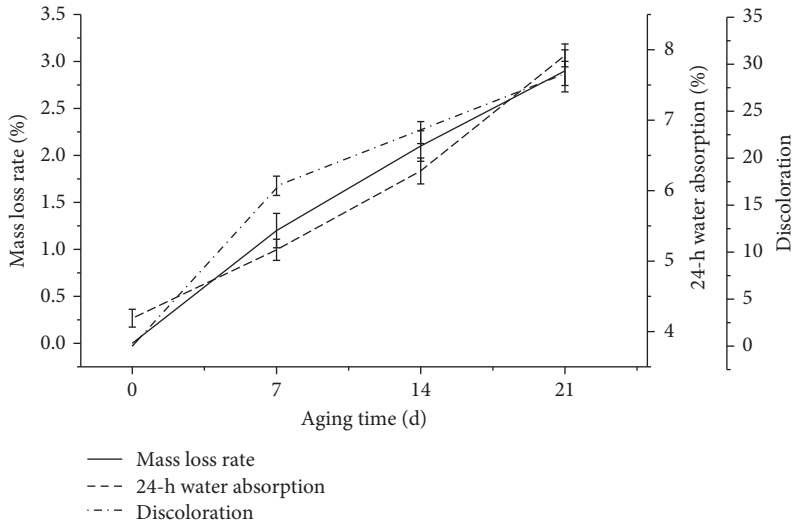

Figure 1: Mass loss rate, 24 h water absorption, and discoloration of the composites.

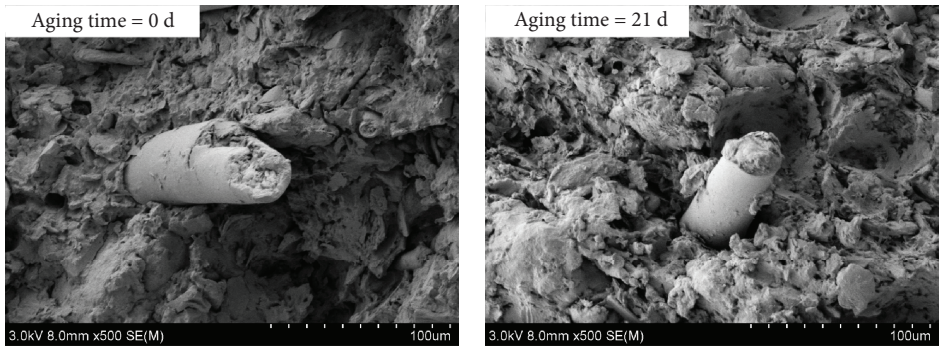

(a) (b)

Figure 2: SEM micrographs of the tensile fracture surfaces of the composites.

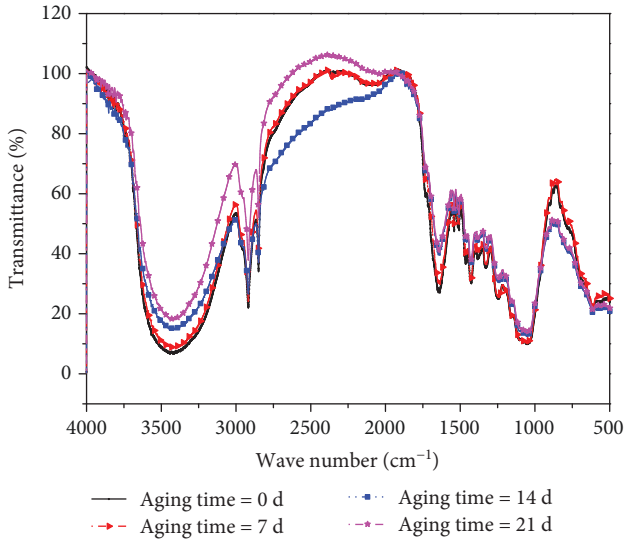

Figure 3: FTIR spectra of the composites.

the stress transfer from the matrix to the fibers. It is thus easier to accumulate stress, and stress damage was triggered. Furthermore, water molecules played a role as a "plasticizer" for the plant cellulose, which resulted in the free movement of cellulose molecules, and the deformation resistance ability of the cellulose structure was broken [30].

3.5. Thermogravimetric Analysis of the PVC/RHF Composites. The curves of the thermogravimetric analysis (TGA) investigation for the PVC/RHF composites under different aging times were examined, as shown in Figure 5, as well as the pyrolysis characterization data of the composites, which are presented in Table 6. There are two stages in the process of weight loss. In the first stage, a rapid weight reduction occurred at 255–325°C (mass reduction 48-50%), which included the pyrolysis of the lignocellulose and the elimination reaction of the HCl in the PVC. The steady stage was controlled at 325–440°C. This process mainly resulted in further pyrolysis of the lignin. In the second stage, a slow weight reduction occurred at 440-500°C (mass reduction 17-20%), which included the degradation of the remaining HCl and

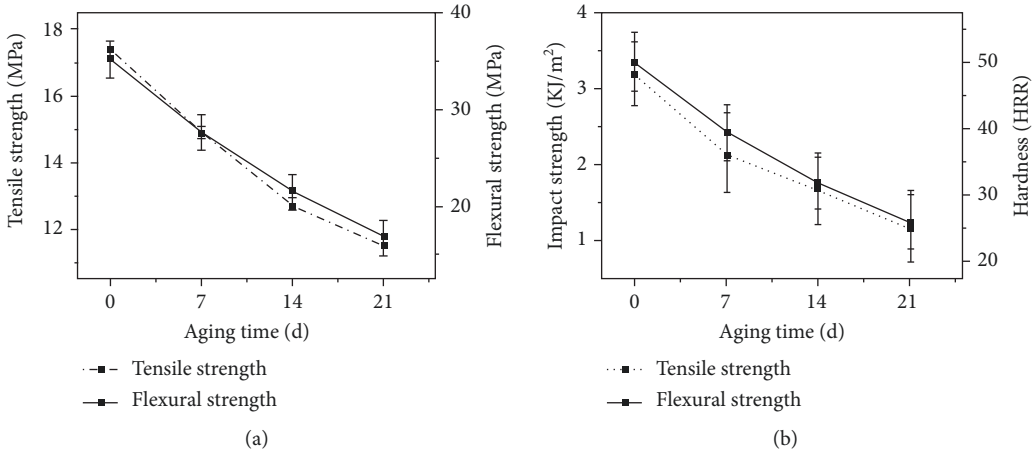

Figure 4: Physical and mechanical properties of the PVC/RHF composites.

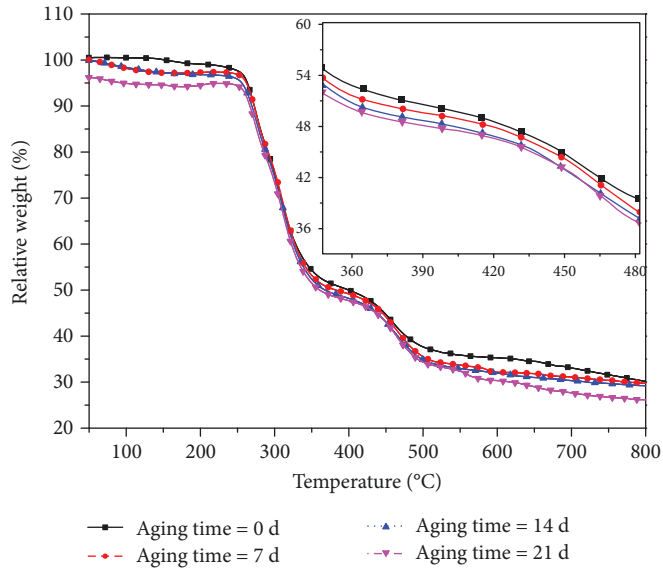

Figure 5: Thermogravimetric curves of the composites.

the broken conjugated double bond in the PVC chain. The degradation of residual substances generally occurred at the beyond of 500°C.

The pyrolysis temperature of the first stage decreased with increasing soil aging time. The trend of the second stage was similar to that of the first stage; therefore, long soil aging leads to a reduction in thermal stability. The presence of interfacial microcracks limited the heat transfer from the PVC matrix (low heat resistance ability) to the fibers (high heat resistance ability). In addition, the mass reduction and residual mass (the first and second stages) of the composites had a decreasing trend with increasing soil aging time. The hemicellulose and lignin of the rice husk fibers were gradually removed in the high-temperature and high-moisture environment; the removal amount had a positive correlation with the soil aging time. The disappearance of hemicellulose and lignin was proven by the FTIR curves.

3.6. Thermal Expansion Properties of the Composites. The high LCTE of the composites had a negative influence in outdoor applications. To better investigate the thermal properties of the PVC/RHF composites with different soil aging periods, the LCTE curves of the PVC/RHF composites with three aging periods were examined, as shown in Figure 6.

The LCTE of the composites is affected by the interaction of the high LCTE of the PVC matrix and the low LCTE of the RHF. The LCTE value of the composites exhibited an obvious increasing trend with increasing soil aging time. As indicated by the LCTE curve, when the soil aging time reached 21 d, the LCTE of the composites increased to 29.98, because many fibers were pulled out from the matrix; the proportion of the fibers and matrix decreased, and microcracks increasingly occurred at the interface. This cannot cause a mechanical and thermal limit on the polymer chain during the heating period [31]. In

Table 6: Pyrolysis characterization data of the PVC/RHF composites.

Aging time (d)	Pyrolysis process						
	First stage Temperature (°C)		Mass reduction (%)	Second stage Temperature (°C)		Mass reduction (%)	Residual mass (%)
	Onset	Termination		Onset	Termination		
0	258.5	321.8	50.53	440.6	462.9	19.65	24.09
7	256.1	319.5	49.77	437.2	459.9	18.83	22.57
14	254.6	316.2	49.69	434.5	456.2	17.36	22.39
21	251.3	312.9	48.50	429.7	451.6	17.04	21.74

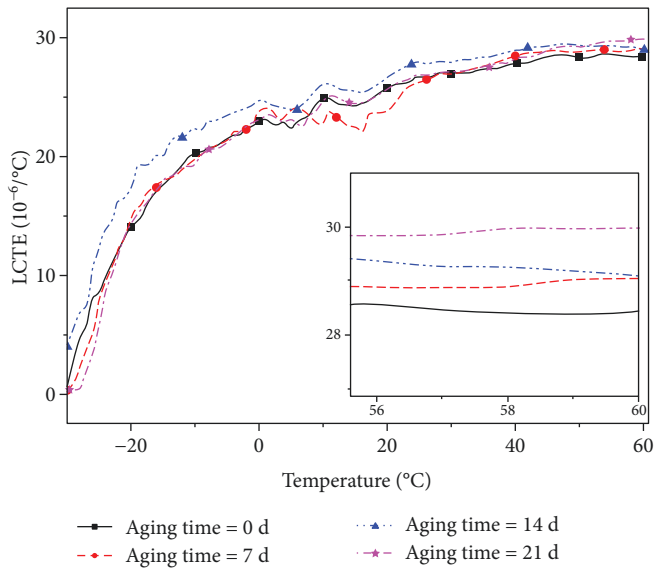

Figure 6: LCTE curve of the composites.

addition, the disappearance of the lignin prevents the covalent and hydrogen bonds from cross-linking with the cellulose and hemicellulose [32], and the thermal expansion behavior becomes more serious; thus, the LCTE of the composites becomes larger than that of the original composites. There is no doubt that better interfacial bonding may decrease the thermal expansion properties of the composites under the soil aging condition.

4. Conclusions

This study mainly investigated the effect of accelerated soil aging on the biodegradation performance of RHF-reinforced PVC composites at different aging periods. Three important conclusions are drawn from the results:

(a) The worst soil aging condition was confirmed through an orthogonal experiment. The soil temperature, pH, moisture content, and porosity weakened the soil aging resistance of the composites. The worst soil aging condition was as follows: soil temperature of 65°C, soil pH of 2.5, soil moisture content of 45%, and soil porosity (ratio of thick and thin) of 3 : 7

(b) The chromatic aberration, mass loss rate, and 24 h water absorption increased following the soil aging experiment. SEM images showed that the interfacial adhesion was weakened with increasing soil aging time, and the fiber was not coated with the plastic matrix. The increased microcracks led to the reduction of tensile strength, flexural strength, impact strength, and hardness. The disappearance of hemicellulose and lignin caused an increased mass loss rate

(c) The pyrolysis temperature, mass reduction, and residual mass (the first and second stages) of the composites had a decreasing trend with increasing soil aging time, but the LCTE value of the composites increased. This may result in poor interfacial adhesion and the disappearance of hemicellulose and lignin; the latter has been proven by the FTIR curves

Data Availability

All data included in this study are available from the corresponding author upon request.

Conflicts of Interest

The authors declare that they have no conflicts of interest.

Acknowledgments

This work was financially supported by the National Key Technology Support Program (2011BAD20B202-2) and the Fundamental Research Funds for the Central Universities (Y0201800586).

References

[1] J. George, M. S. Sreekala, and S. Thomas, "A review on interface modification and characterization of natural fiber reinforced plastic composites," *Polymer Engineering & Science*, vol. 41, no. 9, pp. 1471–1485, 2001.

[2] A. E. Toghyani, M. Amraei, S. Matthews, J. Varis, T. Karki, and X. L. Zhao, "Effect of strain rate and temperature on press forming of extruded WPC profiles," *Composite Structures*, vol. 180, pp. 845–852, 2017.

[3] W. Frącz and G. Janowski, "Analysis of fiber orientation in the wood-polymer composites (WPC) on selected examples," *Advances in Science and Technology Research Journal*, vol. 11, no. 3, pp. 122–129, 2017.

[4] S. Kazemi Najafi, "Use of recycled plastics in wood plastic composites – a review," *Waste Management*, vol. 33, no. 9, pp. 1898–1905, 2013.

[5] É. Hillig, I. Bobadilla, R. Gonçalves, and D. F. Llana, "The influence of wood polymer composite (WPC) specimen composition and dimensions on wave propagation," *European Journal of Wood and Wood Products*, vol. 76, no. 4, pp. 1153–1164, 2018.

[6] C. Hoffmann, M. Lang, P. Heidemeyer, M. Bastian, K. Fischer, and M. Sonntag, "Foam extrusion of PP-based wood plastic composites with chemical blowing agents and the Celuka technique," *Journal of Cellular Plastics*, vol. 53, no. 6, pp. 623–638, 2017.

[7] C. Mei, X. Sun, M. Wan, Q. Wu, S.-J. Chun, and S. Lee, "Coextruded wood plastic composites containing recycled wood fibers treated with micronized copper-quat: mechanical, moisture absorption, and chemical leaching performance," *Waste and Biomass Valorization*, vol. 9, no. 11, pp. 2237–2244, 2018.

[8] S. Chaudemanche, A. Perrot, S. Pimbert, T. Lecompte, and F. Faure, "Properties of an industrial extruded HDPE-WPC: the effect of the size distribution of wood flour particles," *Construction and Building Materials*, vol. 162, pp. 543–552, 2018.

[9] Q. Zhao, X. Li, and J. Gao, "Aging of ethylene–propylene–diene monomer (EPDM) in artificial weathering environment," *Polymer Degradation and Stability*, vol. 92, no. 10, pp. 1841–1846, 2007.

[10] L. H. Staffa, J. A. M. Agnelli, M. L. de Souza, and S. H. P. Bettini, "Evaluation of interactions between compatibilizers and photostabilizers in coir fiber reinforced polypropylene composites," *Polymer Engineering & Science*, vol. 57, pp. 1179–1185, 2017.

[11] L. Xuan, G. Han, D. Wang et al., "Effect of surface-modified TiO_2 nanoparticles on the anti-ultraviolet aging performance of foamed wheat straw fiber/polypropylene composites," *Materials*, vol. 10, no. 5, p. 456, 2017.

[12] X. Wang, K. Song, and R. Ou, "Effects of carbon black and titanium dioxide on ultraviolet weathering of wood flour-HDPE/lumber composites using multi-phase co-extrusion technology," *BioResources*, vol. 12, no. 3, 2017.

[13] G. Hwang, B. Koltisko, X. Jin, and H. Koo, "Nonleachable imidazolium-incorporated composite for disruption of bacterial clustering, exopolysaccharide-matrix assembly, and enhanced biofilm removal," *ACS Applied Materials & Interfaces*, vol. 9, no. 44, pp. 38270–38280, 2017.

[14] Y.-M. Tseng, S.-Y. Chen, C.-H. Chen et al., "Effects of alcohol-induced human peripheral blood mononuclear cell (PBMC) pretreated whey protein concentrate (WPC) on oxidative damage," *Journal of Agricultural and Food Chemistry*, vol. 56, no. 17, pp. 8141–8147, 2008.

[15] L. Jiang, C. He, J. Fu, and D. Chen, "Wear behavior of wood–plastic composites in alternate simulated sea water and acid rain corrosion conditions," *Polymer Testing*, vol. 63, pp. 236–243, 2017.

[16] L. Jiang, C. He, J. Fu, and X. Li, "Wear behavior of alkali-treated sorghum straw fiber reinforced polyvinyl chloride composites in corrosive water conditions," *BioResources*, vol. 13, no. 2, 2018.

[17] J. W. Kim, D. P. Harper, and A. M. Taylor, "Effect of wood species on water sorption and durability of wood-plastic composites," *Wood and Fiber Science*, vol. 40, pp. 519–531, 2008.

[18] A. L. Catto, L. S. Montagna, and R. M. C. Santana, "Abiotic and biotic degradation of post-consumer polypropylene/ethylene vinyl acetate: wood flour composites exposed to natural weathering," *Polymer Composites*, vol. 38, no. 3, pp. 571–582, 2017.

[19] B. Kržan and J. Vižintin, "Tribological properties of an environmentally adopted universal tractor transmission oil based on vegetable oil," *Tribology International*, vol. 36, no. 11, pp. 827–833, 2003.

[20] J. Guo, Y. Tang, and Z. Xu, "Wood plastic composite produced by nonmetals from pulverized waste printed circuit boards," *Environmental Science & Technology*, vol. 44, no. 1, pp. 463–468, 2010.

[21] M. Reowdecha, C. Sukthaworn, P. Dittanet et al., "Degradation of silica-reinforced natural rubber by UV radiation and humidity in soil," *Key Engineering Materials*, vol. 751, pp. 314–319, 2017.

[22] M. Ghorbani, P. Biparva, and S. Hosseinzadeh, "Effect of colloidal silica nanoparticles extracted from agricultural waste on physical, mechanical and antifungal properties of wood polymer composite," *European Journal of Wood and Wood Products*, vol. 76, no. 2, pp. 749–757, 2018.

[23] Z. G. Wang, Y. C. Zhao, Q. L. Liao, B. Huang, W. X. Sun, and Y. B. Qi, "Spatio-temporal variation and associated affecting factors of soil pH in the past 20 years of Jiangsu province China," *Acta Ecologica Sinica*, vol. 28, pp. 720–727, 2008.

[24] A. Kositchaiyong, V. Rosarpitak, H. Hamada, and N. Sombatsompop, "Anti-fungal performance and mechanical–morphological properties of PVC and wood/PVC composites under UV-weathering aging and soil-burial exposure," *International Biodeterioration & Biodegradation*, vol. 91, pp. 128–137, 2014.

[25] B. K. Segerholm, R. E. Ibach, and M. E. Wålinder, "Moisture sorption in artificially aged wood-plastic composites," *BioResources*, vol. 7, pp. 1283–1293, 2012.

[26] T. Huang, X. P. Chen, X. D. Wang, F. Y. Mi, R. Liu, and X. Y. Li, "Effect of pH value on corrosion behavior of Q235 steel in

an artificial soil," vol. 36, pp. 31–38, 2016, *Journal of Chinese Society for Aging and Protection*.

[27] Y. Guo, D. G. Li, J. J. Li, Y. X. Chen, and F. Fang, "Study on anti-aging properties of two new recycled paper-plastic material/PE composites," *Advanced Materials Research*, vol. 183-185, pp. 1961–1965, 2011.

[28] Y. Chen, *Mechanism of the Formation of Chromophore System of Heat-Induced Color Change of Wood*, Beijing Forestry University, 2012.

[29] W. Wang, Q. Han, X. Li, X. Peng, and W. Qian, "Preparation and characterization of PVC matrix composites with biochemical sludge," *Journal of Polymers and the Environment*, vol. 26, no. 8, pp. 3197–3201, 2018.

[30] H. Dhakal, Z. Zhang, and M. Richardson, "Effect of water absorption on the mechanical properties of hemp fibre reinforced unsaturated polyester composites," *Composites Science and Technology*, vol. 67, no. 7-8, pp. 1674–1683, 2007.

[31] R. Huang, W. Xiong, X. Xu, and Q. Wu, "Thermal expansion behavior of co-extruded wood-plastic composites with glass-fiber reinforced shells," *BioResources*, vol. 7, no. 4, 2012.

[32] Y. Lu, X. Y. Wei, Z. M. Zong, Y. C. Lu, W. Zhao, and J. P. Cao, "Structural investigation and application of lignins," *Progress in Chemistry*, vol. 25, no. 5, pp. 838–858, 2013.